Dynamic properties of two-state lasing quantum dot laser for external optical feedback resistant applications

Jianan Duan*§, Yueguang Zhou†, Heming Huang*, Bozhang Dong*, Cheng Wang† and Frédéric Grillot*‡
*LTCI, Télécom Paris, Institut Polytechnique de Paris, 91120 Palaiseau, France
†School of Information Science and Technology, ShanghaiTech University, Shanghai 201210, China
‡Center for High Technology Materials, The University of New-Mexico, Albuquerque, NM 87106, USA
§jianan.duan@telecom-paris.fr

***Abstract*—This work investigates the dynamics of two-state quantum dot lasers through semi-analytically solving a set of rate equations. Simulations reveal that the occurrence of excited state lasing reduces the damping factor and relaxation oscillation frequency of the laser while increases the linewidth enhancement factor associated to the ground state transition. These results are in good agreement with the experimental observation showing that the quantum dot laser becomes more sensitive to external optical feedback at excited state lasing threshold. This work brings novel insights in the understanding of quantum dot laser physics that are useful for designing feedback resistant lasers in photonic integrated technologies.**

***Index Terms*—Semiconductor lasers, quantum dots, linewidth enhancement factor, external optical feedback.**

I. INTRODUCTION

Silicon photonics has been introduced to achieve high performance and low cost photonic integrated circuits (PICs) [1]. However, the challenge in PICs is the parasitic reflections from on-chip components that feed light back into the laser source and cause strong laser destabilization. As on-chip optical isolators are complicated to fabricate, the development of highly optical feedback resistant laser sources is important. Quantum dot (QD) lasers directly grown on silicon have been shown much higher tolerance to external optical feedback than quantum well lasers, mostly attributing to the small linewidth enhancement factor (α_H-factor) and the high damping factor [2]. However, owing to the slow carrier scattering rate and the unclamped gain dynamics, QD lasers can simultaneously emit on both ground state (GS) and excited state (ES) transitions. The critical feedback level (r_{crit}) is an important criterion, corresponding to the maximum feedback ratio that can be tolerated into a communication system for maintaining an error-free operation. Above r_{crit}, the laser enters the coherence collapse regime which is typically determined at the point where the laser linewidth is significantly broadened. We experimentally found that the r_{crit} of the QD laser strongly depends on the occurrence of the ES, demonstrating that the reflection tolerance is greatly degraded at ES lasing threshold of I_{th}^{ES} [3]. This work is therefore motivated by theoretically explaining this phenomenon. Simulations are in good agreement with the experiments, showing that the damping factor and relaxation oscillation frequency (ROF) significantly decrease while the α_H substantially increases at the ES lasing threshold, which finally affects the laser's resistance against external optical feedback.

(a)

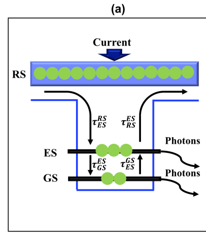

(b)

$$\frac{dN_{RS}}{dt} = \frac{I}{q} + \frac{N_{ES}}{\tau_{RS}^{ES}} - \frac{N_{RS}}{\tau_{ES}^{RS}}(1-\rho_{ES}) - \frac{N_{RS}}{\tau_{RS}^{spon}} + F_{RS} \quad (1)$$

$$\frac{dN_{ES}}{dt} = \left(\frac{N_{RS}}{\tau_{ES}^{RS}} + \frac{N_{GS}}{\tau_{ES}^{GS}}\right)(1-\rho_{ES}) - \frac{N_{ES}}{\tau_{GS}^{ES}}(1-\rho_{GS}) - \frac{N_{ES}}{\tau_{RS}^{ES}} - \Gamma_p v_g g_{ES} S_{ES} - \frac{N_{ES}}{\tau_{ES}^{spon}} + F_{ES} \quad (2)$$

$$\frac{dN_{GS}}{dt} = \frac{N_{ES}}{\tau_{GS}^{ES}}(1-\rho_{GS}) - \frac{N_{GS}}{\tau_{ES}^{GS}}(1-\rho_{ES}) - \Gamma_p v_g g_{GS} S_{GS} - \frac{N_{GS}}{\tau_{GS}^{spon}} + F_{GS} \quad (3)$$

$$\frac{dS_{ES}}{dt} = \left(\Gamma_p v_g g_{ES} - \frac{1}{\tau_p}\right) S_{ES} + \beta_{sp}\frac{N_{ES}}{\tau_{ES}^{spon}} + F_{S_{ES}} \quad (4)$$

$$\frac{dS_{GS}}{dt} = \left(\Gamma_p v_g g_{GS} - \frac{1}{\tau_p}\right) S_{GS} + \beta_{sp}\frac{N_{GS}}{\tau_{GS}^{spon}} + F_{S_{GS}} \quad (5)$$

$$\frac{d\phi_{ES}}{dt} = \frac{1}{2}\Gamma_p v_g\left(g_{GS}\kappa_{ES}^{GS} + g_{ES}\alpha_{ES} + g_{RS}\kappa_{ES}^{RS}\right) + F_{\phi_{ES}} \quad (6)$$

$$\frac{d\phi_{GS}}{dt} = \frac{1}{2}\Gamma_p v_g\left(g_{GS}\alpha_{GS} + g_{ES}\kappa_{GS}^{ES} + g_{RS}\kappa_{GS}^{RS}\right) + F_{\phi_{GS}} \quad (7)$$

Fig. 1. (a) Schematic representation of the electronic structure and carrier dynamics into the quantum dot. (b) Rate equation model.

II. RATE EQUATION MODEL OF QUANTUM DOT LASER

Fig. 1(a) illustrates the schematic of the carrier dynamics of the QD laser, where both electrons and holes are treated as neutral excitons. The QD model consists of a two dimension carrier reservoir RS, a four-fold degenerate ES and a two-fold degenerate GS. The dynamics among the three level is characterised by capture time τ_{ES}^{RS}, relaxation time τ_{GS}^{ES} and escape time τ_{ES}^{GS} and τ_{RS}^{ES}. In addition, carriers in RS, ES and GS are also recombined spontaneously within spontaneous time $\tau_{RS,ES,GS}^{spon}$ respectively. The stimulated emissions are considered to occur in both ES and GS. The dynamics of carrier number $N_{RS,ES,GS}$, the photon number $S_{ES,GS}$, and the phase of the light $\phi_{ES,GS}$ are described by a coupled rate equation model as shown in Fig. 1(b) [4]. Where I is the injected current, q is the elementary charge, $\rho_{RS,ES,GS}$ are the corresponding carrier occupation probabilities in RS, ES, and GS, Γ_p is the optical confinement factor, τ_p is the photon lifetime, β_{sp} is the spontaneous emission factor, and v_g is the group velocity of the light. $\alpha_{ES,GS}$ are the intrinsic α_H-factor of ES and GS, $k_{RS,ES}$ are the contributions of carrier variation in RS and ES to the α_H of GS. $g_{RS,ES,GS}$ represent material gain of each state. $F_{RS,ES,GS}$ are carrier noise sources in RS, ES and GS, respectively. $F_{S_{ES}}$, $F_{S_{GS}}$, $F_{\phi_{ES}}$ and $F_{\phi_{GS}}$ are the corresponding photon and phase noise sources in ES and GS. The damping factor and ROF are extracted from the laser system modulation transfer function, while the α_H is obtained from the frequency noise spectrum [4].

III. RESULTS AND DISCUSSION

Fig.2 shows the bias current dependence of the damping and relaxation oscillation dynamics of the QD laser. At about $0.8 \times I_{th}^{ES}$, the laser is overdamped with a damping factor as

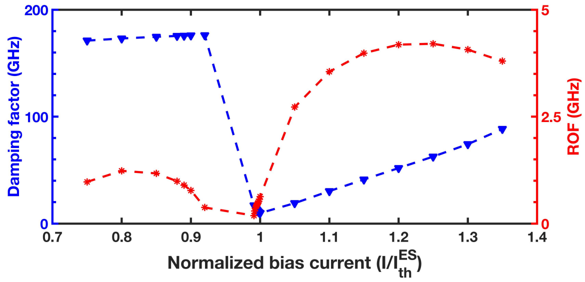

Fig. 2. Current dependence of damping factor (blue) and relaxation oscillation frequency (red).

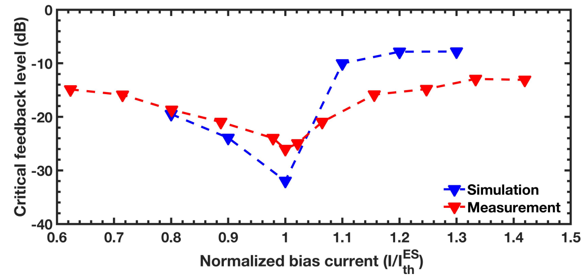

Fig. 4. Critical feedback level (r_{crit}) as a function of the ratio of the bias current normalized to the ES lasing threshold (I/I_{th}^{ES}) for simulation (blue) and measurement (red). Measurement is reproduced from [3].

large as 170 GHz and a ROF of 1.23 GHz. However, along with the increase of the bias current, the damping factor dramatically decreases down to a minimal level at 9 GHz with a ROF of 0.6 GHz at the ES lasing threshold. This large collapse of the damping factor is attributed to the dominant contribution of the spontaneous emission of ES. After the ES lasing threshold, the stimulated emission of ES prevails over the spontaneous emission, which increases the damping factor as well as the ROF. Fig. 3 demonstrates the α_H originates from the GS lasing and ES lasing as a function of the bias current. As shown, the GS α_H increases from 0.7 at $0.2\times I_{th}^{ES}$ to 1.1 at $0.9\times I_{th}^{ES}$, resulting from the increased contribution of carrier variation from ES and RS. Near the ES lasing, the GS α_H dramatically increases to 2.9, which is attributed to the enhanced carrier variation strength in ES associated with the collapsed damping factor [5]. While after ES lasing, the carriers in ES are clamped, thus the carrier variation in ES is suppressed and the damping factor increases again, hence the GS α_H decreases and finally gets saturated around 0.6. By comparison, the ES α_H increases from 0.33 at ES threshold to 0.5 at $1.5\times I_{th}^{ES}$. The r_{crit} can be expressed by the relationship

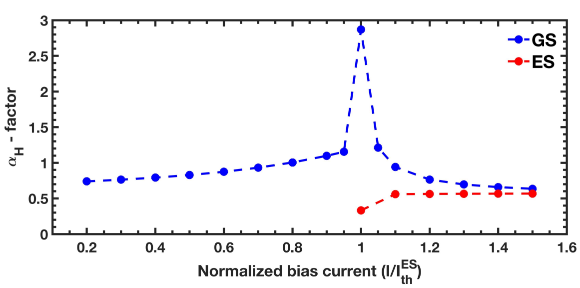

Fig. 3. The α_H-factor as a function of bias currents for GS (blue) and ES (red) transitions, respectively.

[6]: $r_{crit} = \omega_{ROF}^2 R/(1-R)^2(1+\alpha_H^2)\Delta\nu^2$ with ω_{ROF} the angular ROF, R the facet reflectivity coupled to the external cavity, $\Delta\nu$ the free spectral range of the laser. Fig. 4 compares the r_{crit} as a function of the bias current normalized to the ES threshold current (I/I_{th}^{ES}) between the simulation and the measurement. The simulation results qualitatively agree with the measurements, indicating that the QD lasers show strong stability against optical feedback with relative high r_{crit} before the ES lasing occurs. As the bias current increases, the r_{crit} decreases due to the progressive occurrence of the ES and reaches the lowest level at ES threshold. Once the ES lasing occurs, the r_{crit} re-increases with the bias current and the laser returns to the high r_{crit}. However, the simulations do not quantitatively agree with the experiment. This discrepancy can be mostly explained by the model itself, which does not take into account all the peculiar properties of the QD and the lasers have different ES-to-GS ratio. These results demonstrate that the α_H (damping factor respectively) exhibits a local maximum (minimum respectively) value at the onset of the ES lasing which transforms into a local minimum value of the critical feedback level at I_{th}^{ES}. This theoretical analysis is in a good agreement with the experimental observation and tends to prove that QD lasers exhibiting a two-state lasing operation are more sensitive to external optical feedback.

IV. Conclusion

In summary, we theoretically demonstrate that the two-state lasing QD laser exhibits local extrema for the damping, ROF and α_H at the ES lasing threshold. Together, these contributions make the QD laser more sensitive to external optical feedback, which is in good agreement with the prior experimental observation. Overall, this work brings new insights for understanding the physical mechanisms in QD lasers and is useful for designing feedback-insensitive lasers in PICs.
Acknowledgment: This work was supported by National Natural Science Foundation of China (No. 61804095).

References

1 Norman, J. *et al.*, "A review of high-performance quantum dot lasers on silicon," *IEEE Journal of Quantum Electronics*, vol. 55, no. 2, pp. 1–11, 2019.
2 Duan, J. *et al.*, "Dynamic and nonlinear properties of epitaxial quantum dot lasers on silicon for isolator-free integration," *Photonics Research*, vol. 7, no. 11, pp. 1222–1228, 2019.
3 Huang, H. *et al.*, "Analysis of the optical feedback dynamics in InAs/GaAs quantum dot lasers directly grown on silicon," *JOSA B*, vol. 35, no. 11, pp. 2780–2787, 2018.
4 Duan, J. *et al.*, "Carrier-noise-enhanced relative intensity noise of quantum dot lasers," *IEEE Journal of Quantum Electronics*, vol. 54, no. 6, pp. 1–7, 2018.
5 Grillot, F. *et al.*, "Gain compression and above-threshold linewidth enhancement factor in 1.3-μm InAs-GaAs quantum-dot lasers," *IEEE Journal of Quantum Electronics*, vol. 44, no. 10, pp. 946–951, 2008.
6 Binder, J. O. *et al.*, "Mode selection and stability of a semiconductor laser with weak optical feedback," *IEEE Journal of Quantum Electronics*, vol. 25, no. 11, pp. 2255–2259, 1989.